Improvement in electromagnetic interference shielding effectiveness of cement composites using carbonaceous nano/micro inerts

Improvement in Electromagnetic Interference Shielding Effectiveness of Cement Composites Using Carbonaceous Nano/Micro Inerts

Rao Arsalan Khushnood[1]*, Sajjad Ahmad[1], Patrizia Savi[2], Jean-Marc Tulliani[3], Mauro Giorcelli[3], Giuseppe Andrea Ferro[1]

[1] Department of Structural, Geotechnical and Building Engineering (DISEG), Politecnico di Torino, Italy

[2] Department of Electronic and Telecommunication (DET), Politecnico di Torino, Italy

[3] Department of Applied Science and Technology (DISAT), Politecnico di Torino, Italy

* *Corresponding author*

ABSTRACT

The current study is focused to explore a cost effective material for enhancing the electromagnetic interference shielding effectiveness of cement composites. Agricultural residue in the form of peanut and hazelnut shells having little or no economic value was investigated for the subject purpose. These wastes were pyrolyzed at 850 ^{o}C under inert atmosphere and ground to sub-micron-size before utilization with cement. Dispersion of sub-micron-carbonized shell was initially observed in water through visual inspection and later in cement matrix using FESEM micrographs of fractured composites. Results displayed that both carbonized peanut shell (CPS) and carbonized hazelnut shell (CHS) possess excellent ability to get easily dispersed in host medium. The complex permittivity of sub-micron-composites was measured in a wide frequency band (0.2-10 GHz) using a commercial dielectric probe (85070D) and network analyzer E8361A. Due to strong polarization resulting from well dispersed sub-micron carbonized shell inclusions, a significant increase in measured dielectric constant (ε') and dielectric loss (ε'') of cement composites was observed with direct relation to the added content. Numerically evaluated values of electromagnetic interference shielding effectiveness showed remarkable improvement with the addition of sub-micron carbonized shells in cement composites. Maximum increase of 353%, 223%, 126% and 83% was observed in shielding effectiveness at 0.9 GHz, 1.56 GHz, 2.46 GHz and 10 GHz frequencies respectively, by adding only 0.5% CPS by weight of cement, in comparison to the pristine cement samples.

Based on experimental results, it is concluded that the investigated material is highly cost effective (approx. 85% cost saving); very efficient in dispersion as compared to the carbon nanotubes (CNTs) or graphene and quite effective in enhancing the electromagnetic interference shielding properties of resultant cement composites.

Keywords: Cement composites; Dielectric properties; Electromagnetic interference; Shielding effectiveness; Carbonized peanut shell; Carbonized hazelnut shell.

1. Introduction

Besides many advantages, modern developments in electronics especially in wireless and communication systems are contaminating our surroundings with electromagnetic waves (EMWs) pollution. Presence of EMWs in the environment at such an alarming level uplifts the risks of electromagnetic interference (EMI), which may affect the normal functionalization of many electronic and communication devices. Excessive exposure to such radiations is hazardous to human health, as they can enhance the probability of tumors growth in human body [1–4]. Such issues have motivated many researchers and scientists to explore new ways and methods to provide shielding against the severe exposure of EMWs [5–14]. Military stealth technology or LO technology (Low observable technology) also demands new ideas concerning effective electromagnetic shielding.

Cement is the basic building material exhibiting vital role in construction industry. Cement matrix possess poor shielding against EMWs. Some researchers and scientists have done serious efforts to enhance shielding effectiveness of cement composites by making conductive intrusions [15–22]. Wang et al. [23] investigated EMWs absorbing properties of cement nano-composites with varying contents of CNTs and reported maximum absorption at 0.6 wt.% CNTs inclusion in the frequency ranges of 2–8 GHz and 8–18 GHz. Nam et al. [24] analyzed the influence of CNTs dispersion on the electromagnetic interference shielding effectiveness (EMI-SE) of CNTs/cement composites and attained maximum enhancement at 0.94 GHz, 1.56 GHz, 2.46 GHz and 10 GHz frequencies using 0.6 wt.% CNTs and 20 wt.% silica fume. Kong et al. [25] used 3D carbon nanotubes/graphene (CNTs/G) hybrids to achieve adequate dispersion and concluded that these hybrids meet the requirement of

impedance matching, lower EM reflection and improve the EMWs absorption capability of cement matrix.

Although CNTs and graphene possess ideal properties in terms of high specific surface area, low density, high aspect ratio and very high conductivity [26–30] but there are several major concerns that normally restrict their utilization on large scales. One of them is their higher production cost and another is their effective dispersion in cement matrix. Moreover, acid functionalization is often used to improve the adhesion between carbon nanotubes and the cementitious matrix, leading to an increase of the toxicity of CNTs, depending on their degree of catalytic impurities and of a threshold [31].

The literature survey indicates that little attention has been paid on the exploration of cost effective and dispersion free alternatives to improve EMI-SE of cement composites. Therefore, the current study is focused on the utilization of sub-micron-sized, carbonized agricultural residues; which include peanut shell and hazelnut shell to enhance the EM shielding effectiveness of cement composites.

Peanut is one of the most popular and magnificently consumed dry fruit all over the world especially in China and India that are ranked as its top two producers. According to the latest survey of United States Department of Agriculture (USDA), world annual production of peanut is almost 40.18 million metric tons with more than 60% contributions from China and India [32]. Hazelnut is also getting renowned all over the world especially because of its vast usage in many chocolate and ice-cream flavors. Food and agricultural production statistics of United Nations reported that the world's hazelnut production was about 0.91 million metric tons in year 2012, with major part coming from Turkey and Italy that makes about 90% of its annual gross production [33]. Both hazelnut and peanut generate considerable amount of

residues in form of their shells with little to no specific value. Therefore it is important to explore new ways to manage and utilize this bio-waste beneficially.

Peanut shell and Hazelnut shell yield high content of bio char on carbonization [34–37]. An average yield of about 35% was reported for peanut shell at a temperature of around 500 ºC [36], while in case of hazelnut shell it was found more than 40% for the same range of temperature [37]. The economic availability and excellent conversion efficiency of peanut shell and hazelnut shell via pyrolysis, were the two main reasons that motivated the authors to explore their use in cement composites for effective shielding against EMWs.

2. Materials and methods

2.1 Materials and mix proportions

The cement used for the research work was ordinary Portland cement (Type-1, grade 52.5) confirming to the requirements of ASTM C150 [38]. The chemical composition and physical properties of cement as per the product data sheet are presented in Table 1 & 2 [39]. A high range water reducing admixture (HRWRA), based on modified acrylic polymers and confirming to the requirements of UNI EN 934-2:2012 (admixture for concrete, mortar and grout) was used to achieve sufficient workability. Distilled water was utilized for all the mix formulations. The inert sub-micron carbonized particles used for enhancing the shielding effectiveness of the cement composites were obtained from peanut shell and hazelnut shell using the following procedure.

The raw peanut shell (PS) and hazelnut shell (HS) as shown in Figure 1 were washed with tap water and dried in oven for 48 hrs at 105±5 ºC. The washed and dried shells were then pyrolyzed in a quartz reactor at 850 ºC for 1 hour under inert atmosphere. For the provision of inert atmosphere, constant flow of argon was maintained under 0.2 bar pressure in the reactor throughout the pyrolysis process. Carbonized shells were ground in ethanol to sub-

micron scale by ball milling for 24 hrs followed by 2 hrs of attrition milling. The physical properties of ground sub-micron-carbonized shells are given in Table 3.

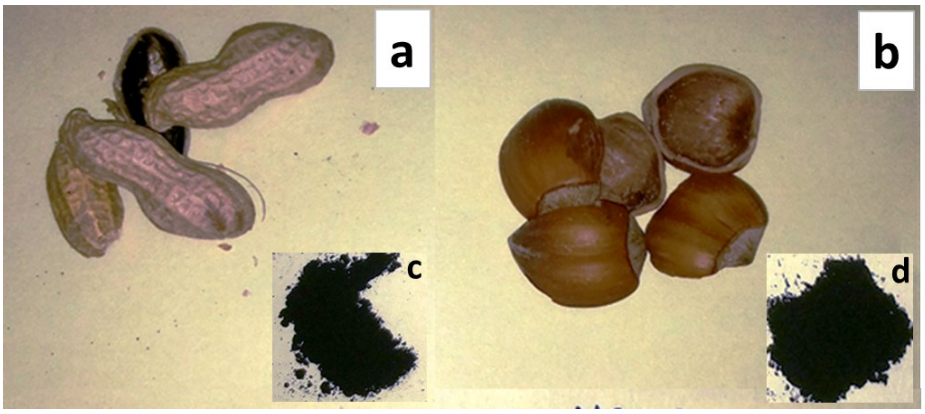

Figure 1: Peanut shell and hazelnut shell in raw form (a & b) and after carbonization and grinding (c & d)

Table 1 Chemical composition of cement

Oxides	CaO	SiO_2	Al_2O_3	Fe_3O_4	SO_3	MgO	K_2O
Content (% by mass of cement)	44	9.50	26.5	2.5	12	1.3	0.60

Table 2 Physical and mechanical properties of cement

Density (g/cm^3)	Color	Specific surface area (cm^2/g)	Compressive Strength (MPa)	
			3 d	28 d
2.80	Light grey	4800	50	65

Table 3 Properties of sub-micron pyrolyzed shells

Sub-micron carbonized shells (CS)	D 50 (nm)	D 90 (nm)	BET surface area (m^2/g)	Density (g/cm^3)
Carbonized peanut shell (CPS)	600	1200	19.4	2.20
Carbonized hazelnut shell (CHS)	750	1300	14.5	2.35

Five mix formulations were prepared including the reference one; detail mentioned in Table 4. Sub-micron carbonized inerts were used as an additive in two proportions i.e. 0.2 and 0.5 wt% of cement. Weight ratios of water and super plasticizer were kept constant at 35% and 1.5% by weight of cement respectively.

137 **Table 4 Mix proportion**

Denotations	Weight compositions (% mass ratio of cement weight)				
	Cement	Water	superplasticizer	(CPS)	(CHS)
CEM	100	35	1.5	0.0	0.0
0P2CPS				0.2	0.0
0P5CPS				0.5	0.0
0P2CHS				0.0	0.2
0P5CHS				0.0	0.5

138

139 **2.2 Preparation**

140 The entire preparation consisted of two steps. First step comprises dispersion of sub-micron
141 carbonized shells (CS) in water with the aid of surfactant and bath sonication for 15 minutes.
142 Second step covers mixing of resultant homogeneous solution with cement using mechanical
143 mixer operated at 440 rpm (slow mixing) for 1.5 min and at 660 rpm (fast mixing) for 2.5
144 min.

145 Mixed cement formulations were poured in associated labeled plastic molds of 6.5 cm in
146 diameter and 1.0 cm in height. The molded specimens were kept in covered plastic box
147 partially filled with water for initial 24 hrs. After that the specimens were demolded and
148 immersed in water. Curing was done at room temperature (20±2 ºC) for 28 days [40]. The
149 cured specimens were dried in oven at 50±5 ºC for 5 days and then stored in air tight bags.
150 Typical cement specimen compared with one euro coin along scale is shown in Figure 2.

151 **2.3 Characterization**

152 To characterize structural order of CS, Raman spectroscopy was carried out by means of
153 Renishaw micro-Raman analyzer with green laser of 514 nm wavelength. Laser beam was
154 focused using 100X objective lens on specimen's surface in 2 µm spot size. The Raman
155 spectrum was restricted in the wavenumber range of 500-3500 cm^{-1}. Field Emission Scanning
156 Electron Microscopy (FE-SEM) along with Energy Dispersive X-Ray (EDX) spectroscopy

was performed to assess morphology, microstructure, elemental composition and dispersion of carbonaceous material in the host cement matrix.

Complex permittivity measurements of cement composites containing sub-micron carbonaceous fillers were performed in the frequency range 0.20-10 GHz with a commercial dielectric sensor (85070D) and a network analyzer (E8361A; see Figure 3). The system was calibrated for water and air before starting measurements. Such measuring system was adopted keeping in view its feasibility to work on specimens with smaller dimensions and it also allows wide-band characterization as well. In all measurements it was tried to ensure perfect contact between sensor probe and specimen's surface. Measurements were taken at six different sites of each single specimen to ensure homogeneity and reduce error margin; reported results are the average of the six measurements.

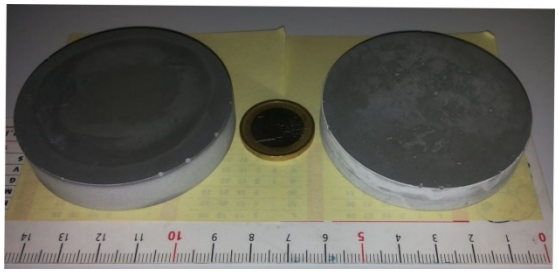

Figure 2 Typical sub-micron cement composite compared with one euro coin

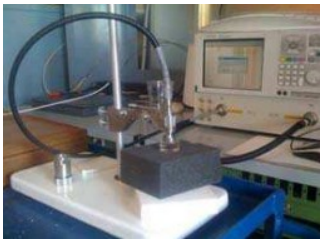

Figure 3 Measurement setup. Agilent sensor (85070D) and Network Analyzer (E8361A)

3. Results and discussions

3.1 Raman spectra analysis

The most relevant wave number range related with Raman spectrum is 1000-1700 cm^{-1}. It is prominent due to the presence of D (defect grade I_D) and G (graphitization grade I_G) bands; which are displayed at approximately 1341 cm^{-1} and 1595 cm^{-1} wavenumbers for CPS while at 1342 cm^{-1} and 1592 cm^{-1} wavenumbers in the case of CHS respectively as shown in Figure 4. The ratio of the two bands is a good indicator related to the quality of carbonaceous filler;

there are quite high structural defects if these bands approach to similar intensity and vice versa. The ratio of I_D to I_G band was similar in the two synthesized products (about 0.85) which indicates that the two materials are equivalent and contain a limited amount of amorphous carbon or of defective graphite crystals in these materials [41].

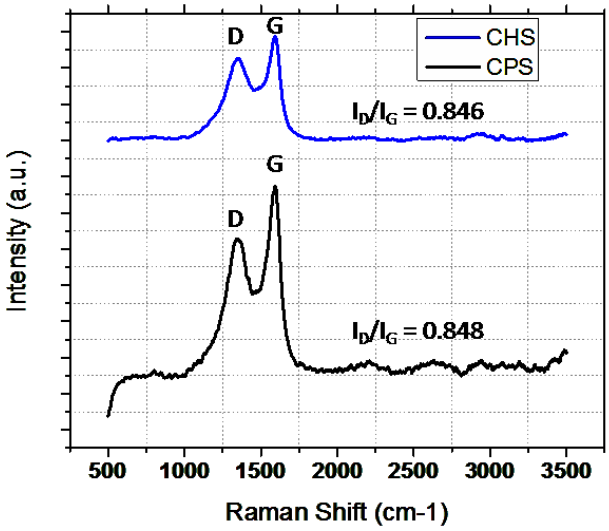

Figure 4 Raman spectra for carbonized peanuts and hazelnuts shells

3.2 Morphology and composition

SEM micrographs as shown in Figure 5 demonstrate that CHS and CPS are in the form of plates/flakes with shape varying from angular to flat and elongated. These plates exhibit glossy and smooth texture with average plate size restricted to less than 800 nm and thickness varying from less than 100 nm up to 300 nm. Such plates seem to be free from entanglement problem as associated with nanotubes and therefore it would be easy to disperse them in cement matrix. As they contain much variety in shape and size so it can be said that they will be quite effective in filling voids of varying size (from gel pores to capillary pores) in cement matrix and thereby enhance its EMI-SE as well as the mechanical performance.

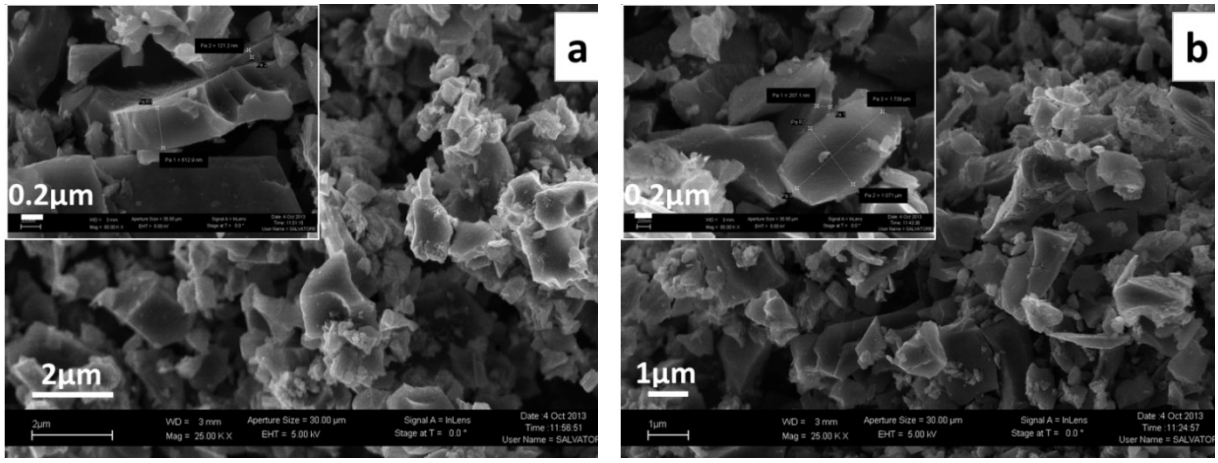

Figure 5 Micrograph of CPS (a) and CHS (b) observed by FE (field emission) SEM

EDX spectrum of CHS and CPS is shown in Figure 6. The spectrum displayed presence of C, Mg, Al, Ca and Si in CS with detailed proportions mentioned in Table 5.

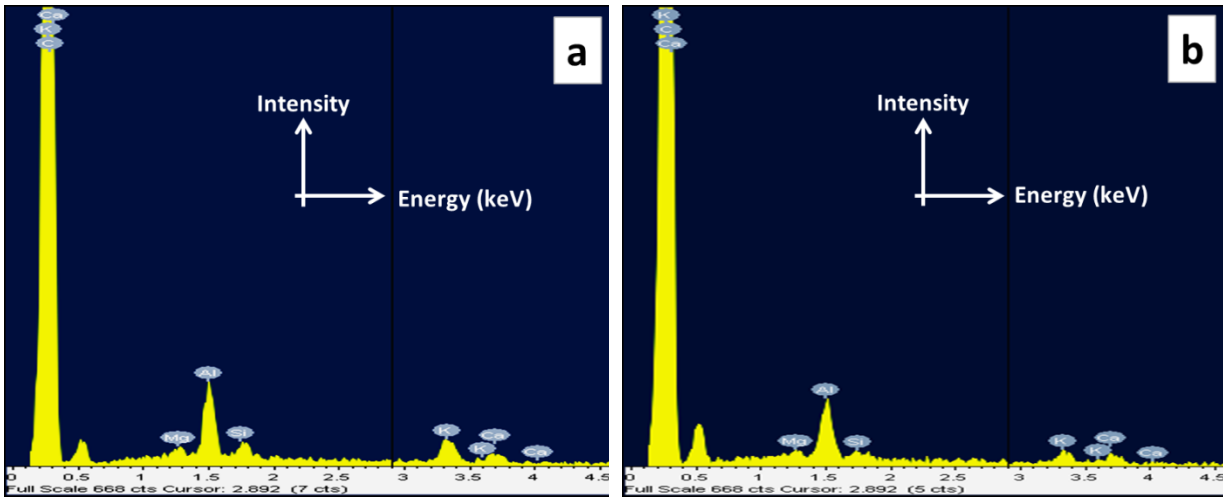

Figure 6 Energy dispersive X-ray spectra of CPS (a) and CHS (b)

Table 5 Elemental composition of CPS and CHS

Elements	CPS (wt%)	CHS (wt%)
C	93.77	87.68
Mg	0.43	0.53
Al	3.01	5.09
Ca	1.20	1.65
Si	0.23	1.14

3.3 Dispersion

It was hypothesized by Nam et. al. [24] that a better dispersion state of CNTs in the cement matrix can bring higher EMI-SE. CS were dispersed in water using ultrasonic treatment and superplasticizer. To demonstrate that a good level of dispersion was achieved a small amount of the solution (water + CS + SP) was diluted with a measured water content (1:5) in a test tube and visually inspected. The color appeared uniform even after one hour of dispersion. If CS were badly dispersed a certain quantity would have deposited at the bottom of the test tube, as in case of 0.5 wt% CNTs dispersed in water for comparison as shown in Figure 7.

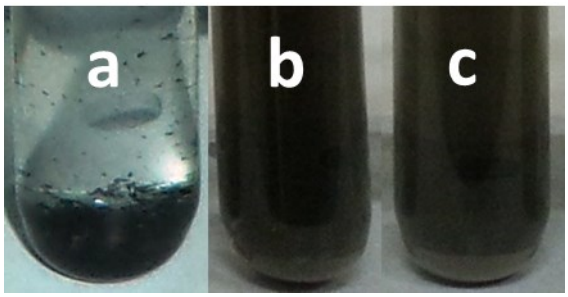

Figure 7 Dispersion level of 0.5wt% CNTs (a), 0p5CPS (b) and 0p5CHS (c) in water after 1hr of dispersion

FE-SEM analysis of fractured cement specimens given in Figure 8 showed better dispersion of CS inside cement matrix. All particles are very well distributed and no signs of agglomeration are visible. Better dispersion results in creation of more and more interfaces which ultimately enhance EMI-SE by increasing absorption loss of EMWs.

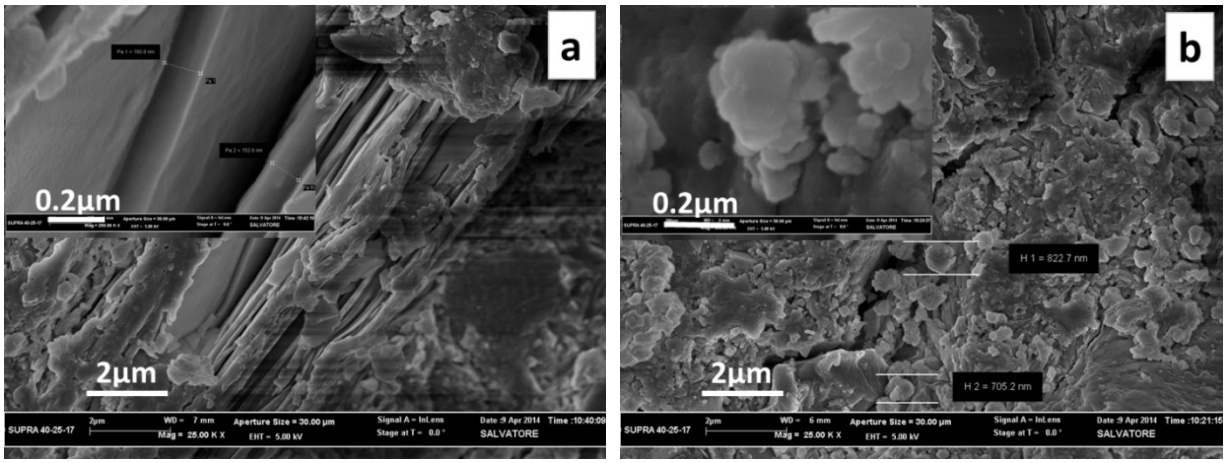

Figure 8 FE-SEM micrographs of 0p5CPS (a) and 0p5CHS (b) fractured cement specimens

3.4 Complex permittivity measurements and analysis

The relative complex permittivity ($\varepsilon_r = \varepsilon' - j\varepsilon''$) was measured using dielectric probe sensor in 0.2-10 GHz frequency range. Figure 9 shows both real (ε') and imaginary (ε'') parts of permittivity as a function of frequency for cement composites with and without CS inclusions. The real part refers to the content of energy stored by material when exposed to external electric field while imaginary part is the measure of dissipated or lost energy. An appreciable increment was observed in the values of real and imaginary permittivity on induction of filler in cement matrix.

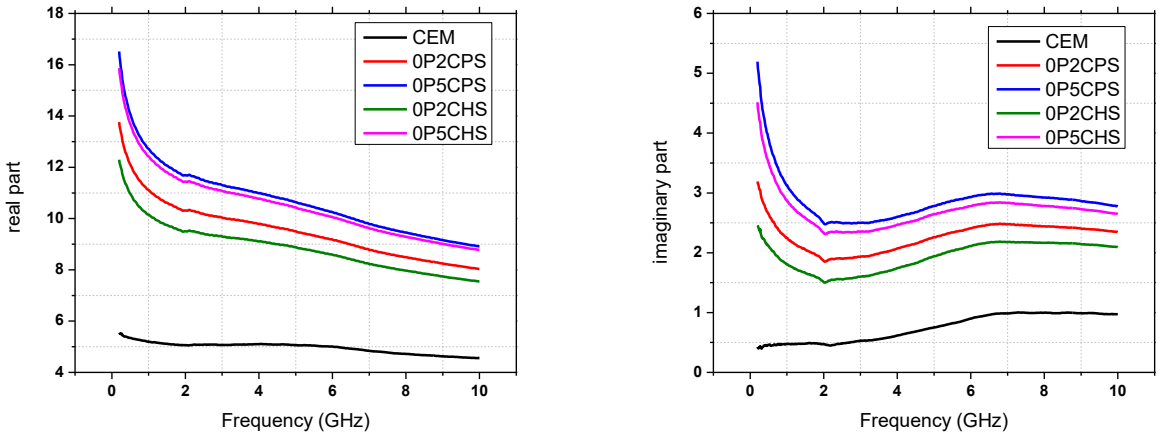

Figure 9 Complex permittivity of pure cement paste and cement composites with varying contents of CPS and CHS.

Dielectric performance of a material depends upon its ionic, electronic, orientation and space charge polarization. Ionic polarization is inversely related to frequency of EMWs with nominal decrease observed at high frequencies. This is the reason why ε' and ε'' reduce on increase in frequency of applied EMWs. Since CS contain carbon (C > 85% see Table 5) which possesses free electrons and bound charges that account for encouraging strong orientational polarization. Inclusion of very well dispersed CS in an insulating medium like cement results in the formation of more interfaces with ultimate increase in space charge

polarization. All these factors contributed to enhance both dielectric constant (ε′) and dielectric loss (ε″) of cement composites containing CS; with direct relation to the added content.

3.5 EMI shielding effectiveness (numerical results)

Shielding effectiveness (SE) is defined in decibels (dB) and mathematically expressed as [19]:

$$SE_{dB} = R_{dB} + A_{dB} + M_{dB} \qquad (1)$$

The mathematical expression of SE clearly demonstrates its dependence upon three major losses occurring while propagation of EMWs through the medium. R_{dB} is termed as reflection loss which occurs due to reflection of EMWs at the material's interfaces. A_{dB} is absorption loss of the wave as it proceeds through the barrier with strong relation to its thickness (t) and skin depth (δ). Skin depth is defined as the material's thickness which can reduce the power of EMWs by a factor of 1/e from its original power during propagation and it is given by following relation:

$$\delta = 2/\sigma\omega\mu \qquad (2)$$

Here σ, μ and ω are the electrical conductivity, magnetic permeability of the material and angular frequency respectively. There is some additional effect on total SE due to re-reflections and transmissions phenomena of EMWs during their propagation through the barrier; known as multiple reflection loss M_{dB} and can be neglected if SE exceeds 10 dB [42].

Total SE along with the three major contributors i.e. R_{dB}, A_{dB} and M_{dB} was numerically evaluated in the frequency range of 0.2-10 GHz based on measured values of dielectric constant (ε') and dielectric loss (ε''). Matlab script was used considering a sample material with a thickness greater than skin depth ($t > \delta$). In the calculations conductivity, permeability and complex permittivity are given by following set of equations respectively:

$$\sigma = \varepsilon'' \omega \varepsilon_o \qquad (3)$$

$$\mu = \mu' \mu_o \qquad (4)$$

$$\varepsilon = \varepsilon' \varepsilon_o \qquad (5)$$

R_{dB}, A_{dB} and M_{dB} were calculated according to following expressions:

$$R_{dB} = 20 * \log_{10} \left| \frac{(Z_O + Z_m)^2}{4 * Z_O Z_m} \right| \qquad (6)$$

$$A_{dB} = 20 * \log_{10} \left| e^{\frac{t}{\delta}} \right| \qquad (7)$$

$$M_{dB} = 20 * \log_{10} \left| 1 - \left[\left(\frac{Z_O - Z_m}{Z_O + Z_m} \right)^2 * e^{-\frac{2t}{\delta}} * e^{-i*2*\beta*t} \right] \right| \qquad (8)$$

Where Z_o and Z_m are the characteristic impedance of free space and barrier material respectively given as.

$$Z_O = \sqrt{\mu_O / \varepsilon_O} \qquad (9)$$

μ_o and ε_o correspond to permeability and permittivity of free space

$$Z_m = \sqrt{\frac{i * \omega * \mu}{\sigma + (i * \omega * \varepsilon)}} \qquad (10)$$

α and β being the propagation factors of shield are related to its propagation constant γ as:

$$\gamma = \sqrt{i\omega\mu[\sigma + (i\omega\varepsilon)]} = \alpha + i\beta \qquad (11)$$

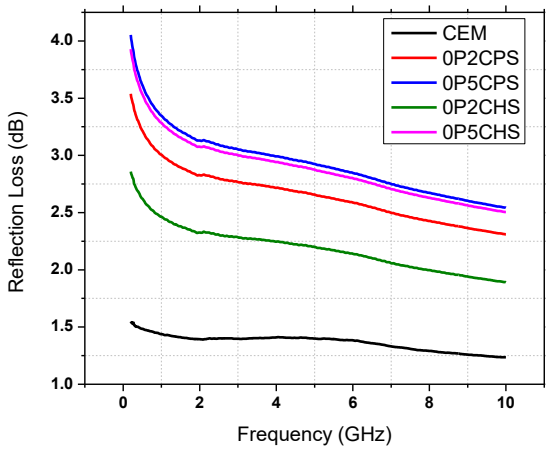

(a) EMW reflection loss of a 10mm thick cement composite sample with and without CS inclusions

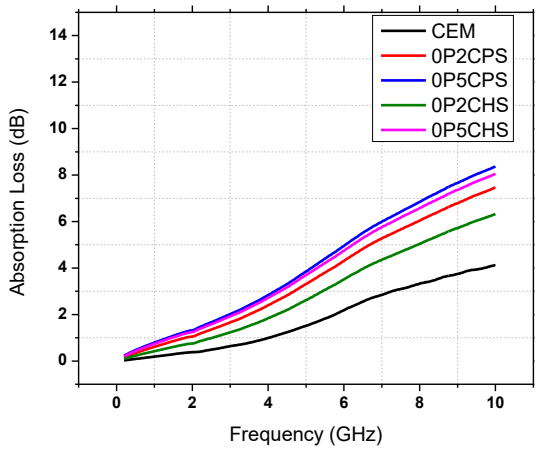

(b) EMW absorption loss of a 10mm thick cement composite sample with and without CS inclusions

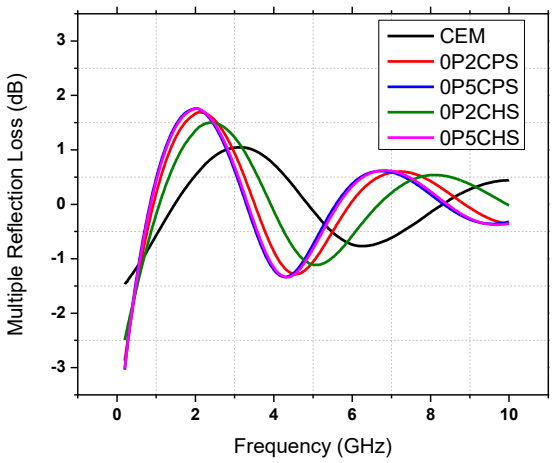

(c) EM wave multiple reflection loss of a 10mm thick cement composite sample with and without CS inclusions

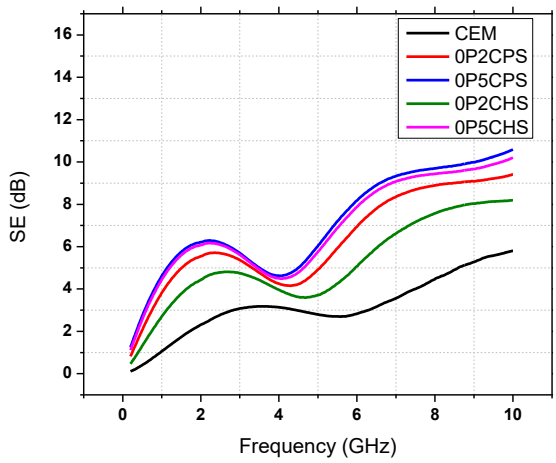

(d) Total shielding effectiveness of a 10mm thick cement composite sample with and without CS inclusions

Figure10 Variation in EMWs Reflection (a), Absorption (b), Multiple reflections (c) and resultant EMI SE (d) of cement nano-composites as a function of frequency

Figure 10 shows that inclusion of both CPS and CHS in cement composites increases their SE and related losses in 0.2-10 GHz frequency range with direct proportionality to the added amount. The observed enhancement pattern of EMI-SE attained on addition of the two CS is almost similar with slightly better results observed in case of CPS; which may be associated to its relatively high specific surface area (Table 1) in comparison to CHS. Another

explanation maybe also due to a higher number of particles distributed within the cementitious matrix, considering that CS additions were done in weight with respect to cement and that CPS have a slightly lower density with respect to CHS, but particles diameter are rather similar.

To have a better evaluation of results, total SE of all five formulations were compared at four different frequencies of 0.94 GHz (frequency of GSM mobiles), 1.56 GHz (frequency of GPS communication devices), 2.46 GHz (frequency of microwave ovens), and 10.0 GHz (frequency of radio communication devices) as done by Nam et al [24]. Figure 11 shows that maximum increase by 353% in SE of cement sub-micron composites was observed on addition of 0.5 wt% CPS at 0.9 GHz frequency. This percentage reduces to 223%, 126% and 83% as we proceed towards high frequency values of 1.56 GHz, 2.46 GHz and 10 GHz, respectively. In case of 0.5 wt % CHS inclusions, a similar patterned increase of 335%, 214%, 122% and 76% was achieved at the four specified frequencies in comparison to reference specimens.

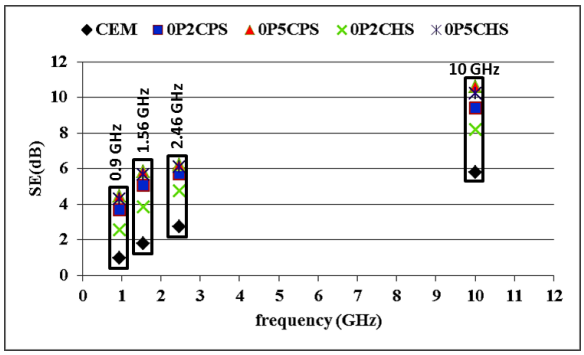

Fig 11 EMI SE of cement sub-micron-composites at specific frequency points with variation of CPS or CHS weight ratios added in cement matrix materials

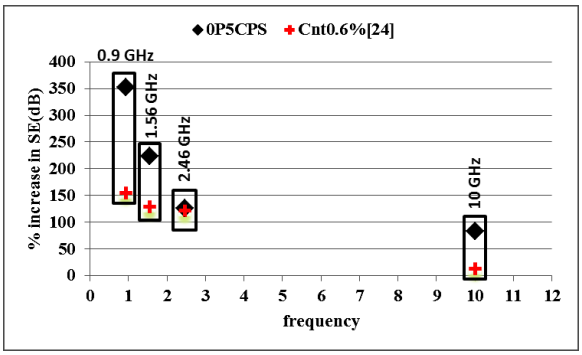

Fig 12 EMI SE comparison of cement sub-micron-composites containing 0p5CPS and 0.6wt% CNTs at specific frequency

Total increase in SE and associated components on adding merely 0.5 wt% CS in cement composites is much higher in comparison to the ones reported by other researcher using expensive CNTs in same content along with heavy amount of costly dispersants [15,24]. To

make the comparison more significant, percentage increase in SE of cement sub-micron composites at the four prescribed frequencies using 0.5 wt% CPS (achieved by authors) was compared with 0.6 wt% CNTs [24] in Figure 12. Comparison shows maximum enhancement on addition of 0.5 wt% CPS in cement composites due to its much better dispersion in water (Figure 7) and then in cement matrix (Figure 8). Nam et al [24] also reported much better results of shielding effectiveness on effectively dispersing CNTs in cement with the addition of 20 wt% silica fume.

4. Cost comparison

To have an idea related to percent reduction in cost on utilizing CS instead of CNTs in preparing one cubic meter cement grout; cost analysis was performed as per the purchased price from the market (as of June 2014). Formulations containing 0.5 wt% additive fillers were selected as they attained much enhanced EMI-SE in comparison with pure cement composites. Based on Eq 12, detailed calculations of quantities and associated expenses are summarized in Table 6. After analysis, it appears that CS inclusions reduce the cost by approx. 88.5% in comparison with corresponding CNTs/cement composites.

Density of CNTs = 2.05 g/cm^3 [43]

Density of SP (assuming Mapei SP1) = 1.09 g/cm^3 [44]

Density of dispersant (assuming gumarabic) = 1.35 g/cm^3 [45]

$$1 = \left(\left(\frac{c}{density\ of\ c}\right) + \left(\frac{wt\ of\ water\ (0.35c)}{density\ of\ water}\right) + \left(\frac{filler\ content\ (0.005c)}{density\ of\ nano\ filler}\right) + \left(\frac{SP\ wt\ (0.015c)}{SP\ density}\right) + \left(\frac{disp\ wt\ (6*CNTs)}{disp\ density}\right)\right) + 0.02\ (air) \qquad (12)$$

Table 6 Comparison of cost analysis

Materials	Unit Price ($)*	CEM		0p5CNTs		0p5CPS		0p5CHS	
		Quantity /m^3	Price ($)	Quantity /m^3	Price ($)	Quantity /m^3	Price ($)	Quantity /m^3	Price ($)
Cement (kg)	0.15	1359.4	203.9	1314.4	201.2	1355.1	203.3	1355.4.	203.3
CNTs (kg)	2000 [46]	-	-	6.57	13140	-	-	-	-
PS (kg)	0.01	-	-	-	-	6.78	0.07	-	-
HS (kg)	0.02	-	-	-	-	-	-	6.78	0.14
SP (kg)	100	20.4	2040	19.7	1970	20.3	2030	20.3	2030
Dispersant (kg)	110	-	-	39.4	4336	-	-	-	-
Processing cost (CS)	5.0	-	-	-	-	6.78	33.9	6.78	33.9
Total cost	-	-	2243.9	-	19647.2	-	2267.3	-	2267.4
Percent Increase (ref CEM)	-	-	100.0	-	776	-	1.08	-	1.08
Percent Reduction (ref 0p5 CNTs)				-	0.0	-	88.5	-	88.5

* $ stands for US dollars

5. Conclusions

A new type of cost effective material in the form of cement composites containing carbonized agricultural residue (comprising CPS and CHS) was proposed for shielding against EMWs. CS/Cement composites were prepared in two different proportions of 0.2 wt% and 0.5 wt%. Visual inspection of pre-dispersed CS in water and FE-SEM analysis of fractured composite specimens showed their excellent dispersion capability in host medium. A significant increase in permittivity, both real and imaginary parts, was observed in 0.2-10 GHz frequency range with direct relation to the added content. Maximum increase in EMI-SE of 353%, 223%, 126% and 83% at 0.9 GHz, 1.56 GHz, 2.46 GHz and 10 GHz frequencies was achieved in the case of 0.5 wt% CPS compared to the reference one.

The investigated material was found much efficient for EMI shielding applications, providing advantage of better dispersion, simple manufacture at a much lower cost (cost saving > 85%) compared to the corresponding CNTs based cement composite material. In future the research will be extended to use other agricultural residues and study more wt% addition levels to analyze their suitability for enhancing EMI-SE of cement composites.

Acknowledgement

The authors acknowledge the PhD grant provided by the Higher education Commission (HEC), Pakistan. The authors are very grateful to Dr. Salvatore Guastella for FE-SEM analysis and Dr. Pravin Jagadale for his help in synthesis of carbonaceous micro inerts. Dr. Stefano Broggio (Mapei S.p.A.) and Dr. Fulvio Canonico (Buzzi Unicem) are also gratefully acknowledged for having provided superplasticizer and cement, respectively.

References

[1] C. Beall, E. Delzell, P. Cole, I. Brill, Brain tumors among electronics industry workers., Epidemiology. 7 (1996) 125–130. doi:10.1097/00001648-199603000-00004.

[2] K.W. Andrews, D.A. Savitz, Accuracy of industry and occupation on death certificates of electric utility workers: Implications for epidemiologic studies of magnetic fields and cancer, Bioelectromagnetics. 20 (1999) 512–518.

[3] T.J. Bender, C. Beall, H. Cheng, R.F. Herrick, A.R. Kahn, R. Matthews, et al., Cancer incidence among semiconductor and electronic storage device workers., Occup. Environ. Med. 64 (2007) 30–36. doi:10.1136/oem.2006.029504.

[4] T.L. Thomas, P.D. Stolley, A. Stemhagen, E.T. Fontham, M.L. Bleecker, P.A. Stewart, et al., Brain tumor mortality risk among men with electrical and electronics jobs: a case-control study., J. Natl. Cancer Inst. 79 (1987) 233–238. doi:10.1093/jnci/79.2.233.

[5] B. Dai, Y. Ren, G. Wang, Y. Ma, P. Zhu, S. Li, Microstructure and dielectric properties of biocarbon nanofiber composites., Nanoscale Res. Lett. 8 (2013) 293. doi:10.1186/1556-276X-8-293.

[6] P.P. Kuzhir, A.G. Paddubskaya, S. a Maksimenko, T. Kaplas, Y. Svirko, Microwave absorption properties of pyrolytic carbon nanofilm., Nanoscale Res. Lett. 8 (2013) 60. doi:10.1186/1556-276X-8-60.

[7] V. Eswaraiah, S. Ramaprabhu, Inorganic nanotubes reinforced polyvinylidene fluoride composites as low-cost electromagnetic interference shielding materials., Nanoscale Res. Lett. 6 (2011) 137. doi:10.1186/1556-276X-6-137.

[8] A. Ameli, P.U. Jung, C.B. Park, Electrical properties and electromagnetic interference shielding effectiveness of polypropylene/carbon fiber composite foams, Carbon N. Y. 60 (2013) 379–391. doi:10.1016/j.carbon.2013.04.050.

[9] C.K. Das, P. Bhattacharya, S.S. Kalra, Graphene and MWCNT: Potential Candidate for Microwave Absorbing Materials, J. Mater. Sci. Res. 1 (2012) 126–132. doi:10.5539/jmsr.v1n2p126.

[10] J. Cao, D.D.L. Chung, Coke powder as an admixture in cement for electromagnetic interference shielding, Carbon N. Y. 41 (2003) 2433–2436. doi:10.1016/S0008-6223(03)00289-6.

[11] Z. Fan, G. Luo, Z. Zhang, L. Zhou, F. Wei, Electromagnetic and microwave absorbing properties of multi-walled carbon nanotubes/polymer composites, Mater. Sci. Eng. B. 132 (2006) 85–89. doi:10.1016/j.mseb.2006.02.045.

[12] Z. Fang, C. Li, J. Sun, H. Zhang, J. Zhang, The electromagnetic characteristics of carbon foams, Carbon N. Y. 45 (2007) 2873–2879. doi:10.1016/j.carbon.2007.10.013.

[13] M. Giorcelli, P. Savi, a. Delogu, M. Miscuglio, Y.M.H. Yahya, a. Tagliaferro, Microwave absorption properties in epoxy resin Multi Walled Carbon Nanotubes composites, 2013 Int. Conf. Electromagn. Adv. Appl. (2013) 1139–1141. doi:10.1109/ICEAA.2013.6632420.

[14] N. Zhao, T. Zou, C. Shi, J. Li, W. Guo, Microwave absorbing properties of activated carbon-fiber felt screens (vertical-arranged carbon fibers)/epoxy resin composites, Mater. Sci. Eng. B. 127 (2006) 207–211. doi:10.1016/j.mseb.2005.10.026.

[15] A.P. Singh, B.K. Gupta, M. Mishra, A. Chandra, R.B. Mathur, S.K. Dhawan, Multiwalled carbon nanotube/cement composites with exceptional electromagnetic interference shielding properties, Carbon N. Y. 56 (2013) 86–96. doi:10.1016/j.carbon.2012.12.081.

[16] L. Baoyi, D. Yuping, Z. Yuefang, L. Shunhua, Electromagnetic wave absorption properties of cement-based composites filled with porous materials, Mater. Des. 32 (2011) 3017–3020. doi:10.1016/j.matdes.2010.12.017.

[17] G. Bantsis, S. Mavridou, C. Sikalidis, M. Betsiou, N. Oikonomou, T. Yioultsis, Comparison of low cost shielding-absorbing cement paste building materials in X-band frequency range using a variety of wastes, Ceram. Int. 38 (2012) 3683–3692. doi:10.1016/j.ceramint.2012.01.010.

[18] H. Guan, S. Liu, Y. Duan, J. Cheng, Cement based electromagnetic shielding and absorbing building materials, Cem. Concr. Compos. 28 (2006) 468–474. doi:10.1016/j.cemconcomp.2005.12.004.

[19] Y. Dai, M. Sun, C. Liu, Z. Li, Electromagnetic wave absorbing characteristics of carbon black cement-based composites, Cem. Concr. Compos. 32 (2010) 508–513. doi:10.1016/j.cemconcomp.2010.03.009.

[20] X. Zhang, W. Sun, Microwave absorbing properties of double-layer cementitious composites containing Mn–Zn ferrite, Cem. Concr. Compos. 32 (2010) 726–730. doi:10.1016/j.cemconcomp.2010.07.013.

[21] Q. Liu, B. Cao, C. Feng, W. Zhang, S. Zhu, D. Zhang, High permittivity and microwave absorption of porous graphitic carbons encapsulating Fe nanoparticles, Compos. Sci. Technol. 72 (2012) 1632–1636. doi:10.1016/j.compscitech.2012.06.022.

[22] J.C. Pretorius, B.T. Maharaj, Improvement of electromagnetic wave (EMW) shielding through inclusion of electrolytic manganese dioxide in cement and tile-based composites with application for indoor wireless communication systems, 8 (2013) 295–301. doi:10.5897/IJPS12.081.

[23] B. Wang, Z. Guo, Y. Han, T. Zhang, Electromagnetic wave absorbing properties of multi-walled carbon nanotube/cement composites, Constr. Build. Mater. 46 (2013) 98–103. doi:10.1016/j.conbuildmat.2013.04.006.

[24] I.W. Nam, H.K. Kim, H.K. Lee, Influence of silica fume additions on electromagnetic interference shielding effectiveness of multi-walled carbon nanotube/cement composites, Constr. Build. Mater. 30 (2012) 480–487. doi:10.1016/j.conbuildmat.2011.11.025.

[25] L. Kong, X. Yin, X. Yuan, Y. Zhang, X. Liu, L. Cheng, et al., Electromagnetic wave absorption properties of graphene modified with carbon nanotube/poly(dimethyl siloxane) composites, Carbon N. Y. 73 (2014) 185–193. doi:10.1016/j.carbon.2014.02.054.

[26] M.H. Al-Saleh, W.H. Saadeh, U. Sundararaj, EMI shielding effectiveness of carbon based nanostructured polymeric materials: A comparative study, Carbon N. Y. 60 (2013) 146–156. doi:10.1016/j.carbon.2013.04.008.

[27] P. Savi, M. Miscuglio, M. Giorcelli, A. Tagliaferro, Analysis of Microwave Absorbing Properties of Epoxy MWCNT Composites, Prog. Electromagn. Res. Lett. 44 (2014) 63–69. doi:10.2528/PIERL13102803.

[28] H. Alkhateb, A. Al-Ostaz, A.H.-D. Cheng, X. Li, Materials Genome for Graphene-Cement Nanocomposites, J. Nanomechanics Micromechanics. 3 (2013) 67–77. doi:10.1061/(ASCE)NM.2153-5477.0000055.

[29] D.D.L. Chung, Electromagnetic interference shielding effectiveness of carbon materials, Carbon N. Y. 39 (2001) 279–285. doi:10.1016/S0008-6223(00)00184-6.

[30] Y.-H. Li, J.-T. Lue, Dielectric constants of single-wall carbon nanotubes at various frequencies., J. Nanosci. Nanotechnol. 7 (2007) 3185–8.

[31] A. Figarol, J. Pourchez, D. Boudard, V. Forest, J.-M. Tulliani, J.-P. Lecompte, et al., Biological response to purification and acid functionalization of carbon nanotubes, J. Nanoparticle Res. 16 (2014) 2507. doi:10.1007/s11051-014-2507-y.

[32] USDA-Foreign Agriculture Service, Peanuts area, yield and production, http://www.fas.usda.gov/psdonline/psdreport.aspx?hidReportRetrievalName=BVS&hidReportRetrievalID=918&hidReportRetrievalTemplateID=1#ancor, [accessed on 06-06-14].

[33] FAOSTAT-Food and Agriculture Organization, Hazelnuts area, yield and production, http://faostat.fao.org/site/567/DesktopDefault.aspx?PageID=567#ancor [accessed on 06-06-14].

[34] J. Nisamaneenate, D. Atong, P. Sornkade, V. Sricharoenchaikul, Fuel gas production from peanut shell waste using a modular downdraft gasifier with the thermal integrated unit, Renew. Energy. (2014) 1–6. doi:10.1016/j.renene.2014.09.046.

[35] C.I.A. Ferreira, V. Calisto, S.M. Santos, E.M. Cuerda-Correa, M. Otero, H. Nadais, et al., Application of pyrolysed agricultural biowastes as adsorbents for fish anaesthetic (MS-222) removal from water, J. Anal. Appl. Pyrolysis. (2015) 1–12. doi:10.1016/j.jaap.2015.01.006.

[36] M.D. Huff, S. Kumar, J.W. Lee, Comparative analysis of pinewood, peanut shell, and bamboo biomass derived biochars produced via hydrothermal conversion and pyrolysis., J. Environ. Manage. 146 (2014) 303–8. doi:10.1016/j.jenvman.2014.07.016.

[37] E. Pu, A.E. Pu, Pyrolysis of hazelnut shells in a fixed-bed tubular reactor : yields and structural analysis of bio-oil, J. Anal. Appl. Pyrolysis. 52 (1999) 33–49. doi:10.1016/S0165-2370(99)00044-3.

[38] ASTMC150, Standard Specification for Portland Cement, in: Annu. B. ASTM Stand. Vol. 04.01 Cem. Lime; Gypsum, 2012.

[39] Buzzi Unicem Next: User manual, Hydraulic binder made with Calcium Sulpho Aluminate clinker, 2014.

[40] K.J. Bois, A.D. Benally, P.S. Nowak, R. Zoughi, S. Member, Cure-State Monitoring and Water-to-Cement Ratio Determination of Fresh Portland Cement-Based Materials Using Near-Field Microwave Techniques, Instrum. Meas. IEEE Trans. 47 (1998) 628–637. doi:10.1109/19.744313.

[41] S.Y. Son, Y. Lee, S. Won, D.H. Lee, S.D. Kim, S.W. Sung, High-Quality Multiwalled Carbon Nanotubes from Catalytic Decomposition of Carboneous Materials in Gas−Solid Fluidized Beds, Ind. Eng. Chem. Res. 47 (2008) 2166–2175. doi:10.1021/ie0711630.

[42] C.R. Paul, Introduction to electromagnetic compatibility, 1992.

[43] C. Grimaldi, M. Mionić, R. Gaal, L. Forró, A. Magrez, Electrical conductivity of multi-walled carbon nanotubes-SU8 epoxy composites, Appl. Phys. Lett. 102 (2013) 223114. doi:10.1063/1.4809923.

[44] Mapei, Dynamon SP1 superplasticizer based on acrylic polymer, Prod. Manual, http//www.mapei.eu/public/COM/products/671_dynamon_sp1_gb.pdf [accessed 23-06-14].

[45] Gum Arabic (9000-01-05), MSDS. Melting Point Boiling Point Density Storage Transport, http://www.chemicalbook.com/ProductMSDSDetailCB1735918_EN.htm [accessed on 23-06-14].

[46] Cheap Tubes, Multi Walled Carbon Nanotubes-MWNTs, http://www.cheaptubes.com/MWNTs.htm#multi_walled_nanotubes-Mwnts_prices [accessed on 24-06-14].